

# LOW TROPOSPHERE WIND MEASUREMENT WITH 1.06 $\mu$ m DOPPLER LIDAR

Zhiqing Zhong<sup>(1)</sup>, Dong Song Sun<sup>(1)</sup>, Bang Xin Wang<sup>(1)</sup>, Hai Yun Xia<sup>(2)</sup>, Jing Jing Dong<sup>(1)</sup>, Xiao Lin Zhou<sup>(1)</sup>, Huan Lin Hu<sup>(1)</sup>, Jun Zhou<sup>(1)</sup>

<sup>(1)</sup>Anhui Institute of Optics and Fine Mechanics, Hefei, 230031 P. R. China, E-mail: zqzhong@aiofm.ac.cn

<sup>(2)</sup>Department of Physics, Soochow University, Suzhou, 215006, P. R. China, E-mail: dssun@aiofm.ac.cn

## ABSTRACT

The 1.06  $\mu$ m Doppler Wind lidar (DWL) is developed to directly detect wind profiles in the low troposphere. Specification and structure of the lidar system are described. The structure and operation principle of its main subassemblies are presented. A description of system is presented along with the examples of lidar line-of-sight wind velocity obtained with DWL system. Recently DWL experiment held in November 2005 at Hefei, Anhui of PRC (31°54'N, 117°09'E). Experimental results have approved the stabilization of the Doppler wind lidar system. Typically clear air wind profiles extended to the altitude of 7 km with 30 m range resolution.

## 1. INTRODUCTION

The global accurate three-dimensional wind profiles have been proved to be able to improve the numerical weather predict more accurately. The atmospheric wind data is obviously one of most important parameters for the applications such as meteorology research, climate study, and the atmospheric sciences. The wind monitoring in clear weather conditions is the extensive interests by the China Meteorological Agency. Comparing to the other wind remote sensors, lidar remote sensing is the only tool that could measure directly Doppler wind in the global region. The European Space Agency (ESA) has been building the ALADIN[1] (the Atmospheric Laser Doppler Instrument) for the mission of the Earth Explorer Core missions of ESA's Living Planet program, which is scheduled for launch in 2008.

Laser Doppler measurements fall into two categories by operating mode: coherent (or heterodyne) detection and direct detection (or incoherent). Coherent detection is based on the heterodyne mixing of the backscatter signal with a local oscillator to generate intermediate frequency signals from which the Doppler shift [2, 3] can be determined. Coherent lidars have been under development and in use for many years, and these systems operate in the IR and near-IR wavelength regions and are dependent on atmospheric aerosols for laser backscatter. For the most regions of the global where the low aerosol density limits to use Mie scattering from aerosols, the backscatter from the molecular atmosphere, i.e., Rayleigh scattering, must be used operating. Doppler wind lidar systems with direct

detection have been developed [4-6], and show a proven technique for measuring winds in the atmosphere.

The direct detection Doppler lidar described in the paper is based on the double edge technique for the low tropospheric wind measurements. The double edge method utilizes two high spectral resolution optical filters located symmetrically about the outgoing laser frequency. The Doppler shifted frequency from aerosol backscatter can be determined by comparing the transmittances of the backscattering light through two filters. Experiments of some direct DWL measurements on wind profiles in the fields have been reported [7-10]. In this paper we describe a Doppler lidar system based on a dual FP etalon. The lidar system uses the double edge etalon optimized for aerosol backscatter Doppler measurement at 1.06  $\mu$ m. The performance of the system presented the wind profiles at the line-of-sight direction obtained in Hefei, China in 2005.

## 2. WIND LIDAR SYSTEM SETUP

The DWL instrument built in Hefei consists of five main units: the laser transmitter, XY-scanner, the receiving optics, the detector and data acquisition, and controller. A schematic of the total lidar system is shown in Fig.1. The parameters of the system are listed in Table 1.

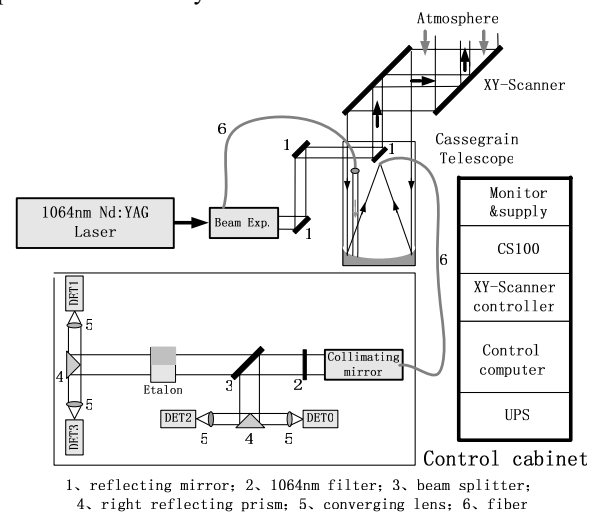


Fig.1. Diagram of the 1.06  $\mu$ m DWL breadboard system.

The DWL system is integrated in a bunk house on the roof of the main building in Anhui Institute of Optics and Fine

Mechanics. The photograph of the complete DWL system is shown in Fig.2. The laser is an injection seeded flashlamp pumped Nd:YAG laser which has a pulse repetition rate of 50 Hz. The pulse length is about 12 ns and the spectral width is less than 90 MHz at the fundamental wavelength of 1.06  $\mu\text{m}$ .

Table 1 System parameters of 1.06  $\mu\text{m}$  DWL

| System parameters                | Value |
|----------------------------------|-------|
| Nd: YAG wavelength/nm            | 1064  |
| Pulse energy/mJ                  | 500   |
| Pulse repetition rate/Hz         | 50    |
| Scanning angle/ $^\circ$         | 45    |
| Receiver diameter /mm            | 300   |
| Receiver full FOV/mrad           | 0.15  |
| Filter bandwidth/nm              | 0.55  |
| Etalon bandwidth/ MHz            | 170   |
| Etalon central distance/ MHz     | 200   |
| Quantum efficiency of detector/% | 2     |
| MCA sampling resolution/ns       | 200   |



Fig.2. Photograph of the 1.06  $\mu\text{m}$  DWL system.

Normally, we operate the laser with energy of 500 mJ/pulse at 1.06  $\mu\text{m}$  for the aerosol measurements. A 30 cm aperture scanner is mounted on the roof to allow access to the atmosphere. The scanner provides full hemispherical pointing using motor driven azimuth and elevation mirrors. We normally operate the scanner pointing at four azimuths: East, South, West and North. The angle of elevation is 45 degrees. The matching 30cm, f/3 Cassegrain telescope is mounted just below the scanner to collect the backscattering signal. The collected signal is coupled directly to an optical fiber. The fiber delivers the signal to

the collimating mirror through which it produces a 48mm diameter collimated light. Between the collimating mirror and beam splitter, mounted a 2 inches and 0.55 nm narrow bandpass interferometer filter. It can limit background induced noise for daytime measurements. Parallel light out of from it is split by a beam splitter into two parts, 20% of which is used as energy monitor, 80% of which is directed along parallel paths through a tunable dual Fabry-Perot etalon. All channel detectors including two etalon channels and two energy monitor channels are operated in photon counting mode.

### 3. PRINCIPLE OF DOPPLER MEASUREMENT

The double-edge technique uses two edges with opposite slopes symmetrically located about the laser frequency, as shown in Fig.3. The laser frequency  $\nu_L$  is located at about the half-width of the two edges. The transmission corresponding to the backscattered laser frequency  $\nu_{PET}$  is then determined. A Doppler shift  $\nu_{DOP}$  will produce from the difference of these transmission measurements in a ratio, as Eq. 1

$$R(\nu) = T_2(\nu) / T_1(\nu) \quad (1)$$

A tunable Fabry-Perot etalon is used as the high spectral resolution edge filter. The 2 inches diameter etalon is divided into two semi-apertures with a small step difference and formed two etalon cavities. Its nominal cavity spacing is about 42.856 mm, and the cavity scanning range is large than 3.5  $\mu\text{m}$ . To obtain etalon transmission curves we linearly scan one of cavity mirrors by a digital stepping controller while assuming the laser frequency stable during the short time scanning.

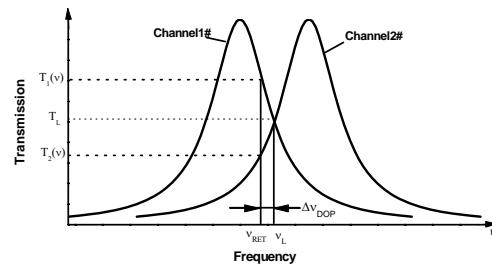


Fig.3. Double-edge schematic diagram.

The etalon transmission curves with the measurements of a seeded cw (continue wave) laser and the pulsed laser has

been reported in [11]. The measured transmission curves are agreed with the designed parameters listed in table 1. In order to inspect the stability of the system receiver, especially the dual FP etalon, a series of transmission measurements in eight days are show in Fig.4. The standard deviations of these measurements for the two channels  $\sigma_1$  and  $\sigma_2$  are about 0.8% and 0.6%, respectively.

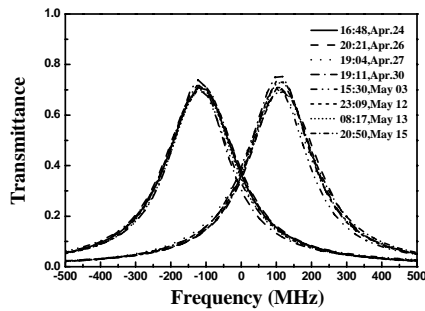


Fig.4. A spectral scan of the etalon transmission measured in eight days.

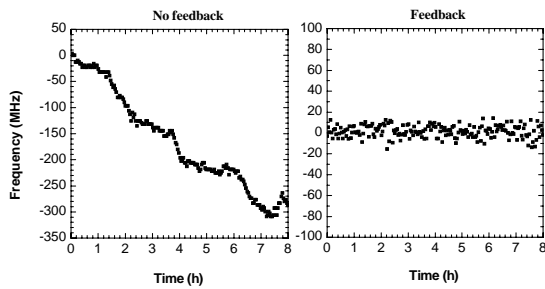


Fig.5. Frequency drift of the etalon measured in eight hours. (a) Without feedback. (b) With feedback.

The laser frequency should be located at the cross point of transmission curves of two etalons, and the stability or drift of the relative location between laser frequency and etalon center may produce wind measurement inaccurate. This frequency drift results from both laser frequency drift and etalon cavity length drift. The frequency drift of them is inspected and measured in eight hours, as shown in Fig.5 where one can find the drift could reach to 300 MHz. A feedback circuit is developed and locks the etalon sharp edge (cross point of dual etalon curves) to the laser frequency. As the relative laser frequency can be decided by the transmission curves of the dual etalons and the etalon transmission curve center can be changed by tuning its cavity, the feedback circuit checks the measured transmissions and produces a bias voltage to tune etalon cavity. In this way the laser frequency will be locked at the cross point of two transmission curves. Fig.5 (b) shows the

long term frequency drift with the feedback, the average is around zero and the standard deviation is about  $\pm 6$  MHz. Experimental results had proved the stabilization of the DWL receiver.

#### 4. WIND MEASUREMENTS

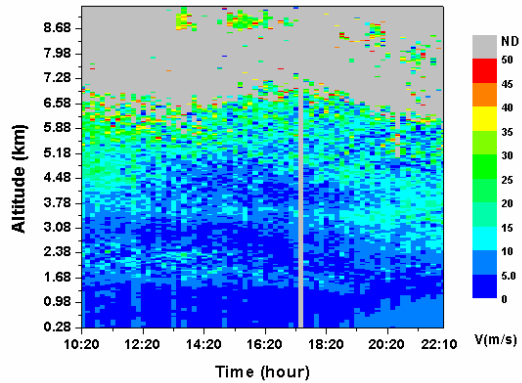


Fig.6. A color plot of ten hours wind profiles measured by Doppler wind lidar from 10:20 to 22:10 of Mar.14, 2006

DWL experiments have been performed since November 2005 at Hefei, Anhui of PRC ( $31^{\circ}54'N$ ,  $117^{\circ}09'E$ ). Over 300 hours of wind velocity data were obtained using DWL system in this experiment. Fig.6 shows the wind velocity field obtained by Doppler wind lidar during ten hours of March 24, 2006. The lidar were pointed at an elevation angle of  $45^{\circ}$  and the bin width is 200 ns. These data are 5000-shots average. Wind velocity is shown as a function of altitude (y-axis) and time (x-axis) with ten minutes interval. The wind velocity in m/s for each altitude interval is mapped to the color scale given on the right. Doppler wind lidar detected profiles of wind speed were obtained to altitudes of as much as 7 km. Long time measurements have proved that DWL lidar system has the capability of unattended automated measurements.

Figure 7 shows a summary of the comparison of wind speed and direction. The Doppler wind lidar measurements are in good agreement with the CINRAD [12]. The CINRAD is a kind of Doppler weather radar. Its basic principle is similar to the WSR-88D in USA. The wind profile is measured by Doppler wind lidar with 30 m line-of-sight resolution. 5000 pulses were averaged for low altitude measurement from 0.28 km to 5.7 km. The profiles of Doppler wind lidar show a mid-level jet at about 3.2 km with a local maximum speed of 25 m/s, and clear evidence of wind shear feature at about 3km. The data from the CINRAD measured with 300 m vertical resolution from

4.3 km to 5.5 km. Both of the lidar and CINRAD show good agreement in this range. A local minimum of 2 m/s in the wind speed was observed at 4.3 km.

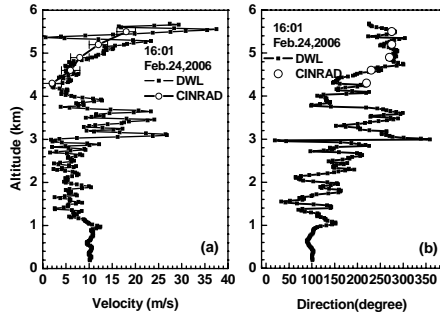


Fig.7. Profiles of wind speed and direction measured by Doppler wind lidar compared with data from CINRAD on February 24, 2006

## 5. CONCLUSION

A ground based Doppler wind lidar using direct detection double edge technique is built and described. The stabilization of the lidar has been proved by long-term Doppler shift measurement of FP etalon and the long-time frequency drift of which is around 0 MHz with feedback. Over 300 hours of wind velocity data were obtained using Doppler wind lidar system in this experiment. The lidar system has been proved to have the capability of unattended automated measurements. Doppler wind lidar detected profiles of wind speed and direction were obtained to altitudes of as much as 7 km. The Doppler wind lidar measurements and the independent CINRAD wind measurements are in good agreement.

## 6. REREFENCES

- [1] Paul Ingmann, ESA Report, SP-1233(4), July(1999).
- [2] F. F. Hall Jr., R. M. Huffaker, R. M. Hardesty and M. E. Jackson, Appl. Opt. 23, (1984).
- [3] R. M. Huffaker, R. M. Hardesty, Proc. IEEE 84, (1996).
- [4] C. Souprayen, A. Garnier, A. Hertzog and A. Hauchecorne, Opt. 38(12),(1999).
- [5] B. M. Gentry, H. Chen, and S. X. Li, Opt. Lett. , 25, 17 (2000).
- [6] J. G. Yoe, M. K. Raja, R. M. Hardesty, W. A. Brewer, SPIE 4893, 2002.
- [7] C. L. Korb, B. Gentry, and C. Y. Weng, Applied Optics, 31(1992).

- [8] B. Gentry and C. L. Korb, Applied Optics, 33(1994).
- [9] C. L. Korb, B. Gentry, and S. X. Li, Applied Optics, 36(1997).
- [10] Bruce M. Gentry, Huailin Chen and Steven X. Li, Optics Letters, 25(2000).
- [11] D. Sun, Z. Zhong, J. Zhou, Optical Review, 12, 5(2005).
- [12] X. Yu, X. Yao and T. Xiong, Meteorologic Publishing House. 2006.